

1 **THE NON-LOCAL AFM WATER-WAVE METHOD FOR**
2 **CYLINDRICAL GEOMETRY***

3 M. G. BLYTH[†] AND E. I. PĂRĂU[‡]

4 **Abstract.** We develop an AFM (Ablowitz-Fokas-Musslimani) method applicable to studying
5 water waves in a cylindrical geometry. As with the established AFM method for two-dimensional
6 and three-dimensional water waves, the formulation involves only surface variables and is amenable
7 to numerical computation. The method is developed for a general cylindrical surface, and we demon-
8 strate its use for numerically computing fully nonlinear axisymmetric periodic and solitary waves on
9 a ferrofluid column.

10 **Key words.** Ablowitz-Fokas-Musslimani method, nonlinear waves, ferrofluid column

11 **AMS subject classifications.** 76B25, 76B10

12 **1. Introduction.** In the classical water wave problem a solution is sought de-
13 scribing an inviscid fluid motion with a free surface. If the fluid motion is irrotational
14 the mathematical problem requires the solution of Laplace’s equation subject to a
15 suitable condition on the bottom in the case of finite depth, or at minus infinity
16 in the case of infinite depth, and subject to Bernoulli’s equation and the kinematic
17 condition at the free surface. Of particular interest is the determination of the free
18 surface itself, and the description of waves propagating along the free surface, their
19 shape, speed, and so on.

20 Numerous analytical approaches have been developed for tackling this problem
21 (for a review see, for example, Lannes [14]). In 2006 Ablowitz *et al.* [1] presented
22 a new non-local formulation which they developed by exploiting a carefully chosen
23 identity for harmonic functions. We shall refer to this as the AFM (Ablowitz-Fokas-
24 Musslimani) method. This was used to re-express the problem in terms of an integral
25 over the free surface to be solved along with Bernoulli’s equation. Accordingly their
26 formulation involves only surface variables and can therefore be solved independently
27 and without reference to the remainder of the flow domain. This new approach has
28 been used, for example, to study the stability of two-dimensional periodic waves on
29 water of finite depth in the presence of gravity (Deconinck & Oliveras [8]) and in
30 the presence of both gravity and surface tension (Deconinck & Trichtchenko [9]), and
31 for bathymetry detection from surface data (Vasan & Deconinck [20]). It has also
32 been extended to include vorticity (Ashton & Fokas [4]) and to two-layer flows (Haut
33 & Ablowitz [13]). In effect the AFM formulation is a surface-variables description
34 of the water waves problem with an implicit Dirichlet-to-Neumann operator. The
35 performance of the AFM method against other Dirichlet-to-Neumann formulations,
36 including the Craig-Sulem operator expansion approach, has been assessed by Wilken-
37 ing & Vasan [21].

38 To date the AFM method has been applied to study two-dimensional and three-
39 dimensional surface waves. In this paper we show how it can be adapted to a cylindri-
40 cal geometry, and we derive the cylindrical analogue of the nonlocal surface integral
41 of Ablowitz *et al.* [1]. By way of demonstration, we illustrate the utility of this

*Submitted to the editors 23rd August 2018.

[†]School of Mathematics, University of East Anglia, Norwich, NR4 7TJ, United Kingdom
(m.blyth@uea.ac.uk).

[‡]School of Mathematics, University of East Anglia, Norwich, NR4 7TJ, United Kingdom
(e.i.parau@uea.ac.uk)

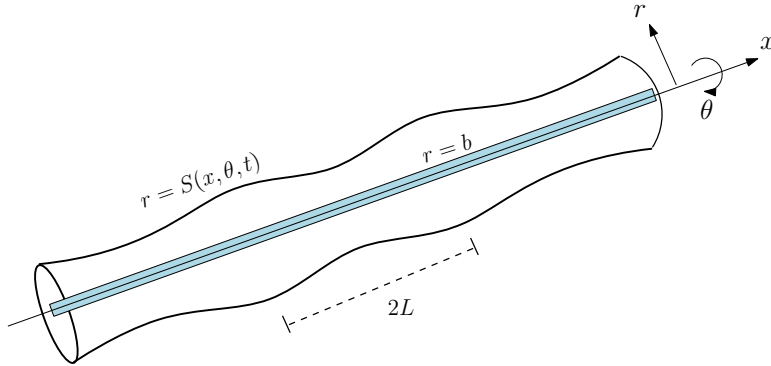


FIG. 1. Sketch of the periodic flow geometry. The domain Ω occupies one wavelength $-L \leq x \leq L$ with $b \leq r \leq S(x, \theta, t)$.

42 formulation for numerically computing fully nonlinear, axisymmetric periodic waves
 43 and solitary waves on a liquid column. Periodic axisymmetric waves on a cylindrical
 44 liquid jet have previously been computed by Vanden-Broeck *et al.* [19] using a fi-
 45 nite difference method. While a cylindrical column will normally tend to disintegrate
 46 into droplets by virtue of the well-known Rayleigh-Plateau instability, if the liquid
 47 in question is a ferrofluid, which is essentially a stable suspension of tiny magnetize-
 48 able particles (e.g. Rosensweig [16]), the Rayleigh-Plateau instability can be resisted
 49 and the column fully stabilised when it is subjected to an azimuthal magnetic field
 50 (Arhipenko & Barkov [3]). Such a field can be generated by placing an electric
 51 current-carrying wire or metal rod along the axis of the column. Nonlinear waves on
 52 the surface of a ferrofluid column stabilised in this way have previously been studied
 53 by Bashtovoi *et al.* [5] and Rannacher & Engel [15] using a weakly-nonlinear model
 54 equation of KdV type. Experiments confirming the possibility of periodic waves and
 55 solitary waves were performed by Bourdin *et al.* [7]. Fully nonlinear solitary wave so-
 56 lutions were computed by Blyth & Părău [6]. We emphasise that it is not our intention
 57 here to further the study of this physical phenomenon per se, rather to demonstrate
 58 the efficacy of the cylindrical AFM formulation for computing such waves.

59 **2. Equations of motion.** We consider a generally unsteady inviscid, incom-
 60 pressible and irrotational axisymmetric fluid motion with velocity $\mathbf{u} = \nabla\phi$, where
 61 $\phi(x, r, \theta, t)$ is the velocity potential with cylindrical polar coordinates (r, θ) and time
 62 t . The velocity potential satisfies Laplace's equation

$$63 \quad (2.1) \quad \nabla^2\phi = 0,$$

64 in the fluid domain Ω , which we take to be cylindrical, occupying the region $b \leq$
 65 $r \leq S(x, \theta, t)$, $-L \leq x \leq L$, $0 \leq \theta \leq 2\pi$ for some given constants $L > 0$ and
 66 $b > 0$. The boundary $r = b$ is assumed to be a solid surface, and the boundary at
 67 $r = S(x, \theta, t)$ is assumed to be a free surface whose particular form is to be determined
 68 as part of the solution to the problem. With a view to later computing travelling wave
 69 solutions we henceforth adopt periodic boundary conditions at the domain ends $x =$
 70 $\pm L$. Solitary wave solutions can be computed within this framework by considering
 71 L to be sufficiently large.

72 Bernoulli's equation holds at the free surface so that

$$73 \quad (2.2) \quad \phi_t + \frac{1}{2} \left(\phi_x^2 + \phi_r^2 + \frac{1}{r^2} \phi_\theta^2 \right) + \frac{\gamma\kappa}{\rho} - V = \mathcal{E}(t),$$

74 at $r = S$, where γ is the surface tension at the free surface, κ is the curvature of the
 75 free surface, ρ is the fluid density, V represents a potential field associated with one
 76 or more body forces per unit mass that are influencing the fluid motion, and $\mathcal{E}(t)$
 77 is the Bernoulli constant. The kinematic condition at the free surface requires that
 78 $D(r - S)/Dt = 0$, where D/Dt is the material derivative, which yields the condition

$$79 \quad (2.3) \quad S_t + \phi_x S_x + \phi_\theta \frac{S_\theta}{S^2} = \phi_r$$

80 on $r = S$. On the solid boundary we enforce the impermeability condition $\phi_r = 0$ at
 81 $r = b$.

82 Our goal is to reformulate the problem in terms of free surface variables only.
 83 Following the approach of Ablowitz *et al.* [1], we start by noting that, if two functions
 84 $\phi(x, r, \theta, t)$ and $\psi(x, r, \theta, t)$ both satisfy Laplace's equation, then it is the case that

$$85 \quad \partial_r(\phi_x \psi_r + \psi_x \phi_r) + \frac{(\phi_x \psi_r + \psi_x \phi_r)}{r} + \frac{1}{r} \partial_\theta \left(\phi_x \frac{\psi_\theta}{r} + \psi_x \frac{\phi_\theta}{r} \right) \\ 86 \quad (2.4) \quad + \partial_x \left(\phi_x \psi_x - \phi_r \psi_r - \frac{1}{r^2} \phi_\theta \psi_\theta \right) = 0 \\ 87$$

88 as can be readily checked by expanding the brackets. The identity (2.4) is in divergence
 89 form which motivates us to introduce the intermediary vector field

$$90 \quad (2.5) \quad \mathbf{a} = \left(\phi_x \psi_x - \phi_r \psi_r - \frac{1}{r^2} \phi_\theta \psi_\theta \right) \mathbf{e}_x + (\phi_x \psi_r + \psi_x \phi_r) \mathbf{e}_r + \left(\phi_x \frac{\psi_\theta}{r} + \psi_x \frac{\phi_\theta}{r} \right) \mathbf{e}_\theta,$$

91 where \mathbf{e}_x , \mathbf{e}_r , and \mathbf{e}_θ are the unit vectors in the x , r , and θ directions respectively.
 92 Choosing ϕ to be the velocity potential and applying the divergence theorem to the
 93 vector field \mathbf{a} over the domain Ω we obtain

$$94 \quad \int_0^{2\pi} \int_{-L}^L S \left[(\phi_x \psi_r + \psi_x \phi_r) - S_x \left(\phi_x \psi_x - \phi_r \psi_r - \frac{1}{S^2} \phi_\theta \psi_\theta \right) \right. \\ 95 \quad (2.6) \quad \left. - \frac{S_\theta}{S^2} (\phi_x \psi_\theta + \psi_x \phi_\theta) \right]_{r=S} dx d\theta - b \int_0^{2\pi} \int_{-L}^L [\phi_x \psi_r]_{r=b} dx d\theta = 0, \\ 96$$

97 where we have enforced the impermeability condition at $r = b$.

98 Inspired by Ablowitz *et al.* [1], we now choose for ψ the particular solution of
 99 Laplace's equation

$$100 \quad (2.7) \quad \psi = e^{i(kx+m\theta)} F(r)$$

101 with

$$102 \quad (2.8) \quad F(r) = [kbK_{m+1}(kb) - mK_m(kb)] I_m(kr) + [kbI_{m+1}(kb) + mI_m(kb)] K_m(kr),$$

103 where I_m , K_m are modified Bessel functions of the first and second kind (e.g. Abramowitz
 104 & Stegun [2]), m is a non-negative integer, and $k = n\pi/L$ for integer $n = \pm 1, \pm 2, \dots$

105 We note that the particular form (2.7) has been devised so that the second integral
106 in (2.6) vanishes identically.

107 Keeping in mind our objective of determining a set of equations of motion in terms
108 of free surface variables only, we introduce the surface potential function $q(x, \theta, t) \equiv$
109 $\phi(x, S, \theta, t)$. By straightforward differentiation

$$110 \quad (2.9) \quad q_x = \phi_x + S_x \phi_r, \quad q_\theta = \phi_\theta + S_\theta \phi_r, \quad q_t = \phi_t + S_t \phi_r,$$

111 where the terms on the right hand sides are evaluated at the surface $r = S$. Utilising
112 these relations together with the kinematic condition (2.3), and assuming (2.7), the
113 integral expression (2.6) becomes

$$114 \quad (2.10) \quad \int_0^{2\pi} \int_{-L}^L S \left[iF(S) \left(kS_t + \frac{m}{S^2} (q_x S_\theta - q_\theta S_x) \right) + q_x F'(S) \right] e^{i(kx+m\theta)} dx d\theta = 0.$$

116 Equation (2.10) represents the central equation of motion and it is expressed purely
117 in terms of surface variables. It is the cylindrical analogue of equation (I) in Ablowitz
118 *et al.* [1].

119 At this point in the interest of simplicity we specialise to axisymmetry and assume
120 from here on that all variables are independent of θ . The particular solution (2.7)
121 reduces to

$$122 \quad (2.11) \quad \psi = kb \left(K_1(kb) I_0(kr) + I_1(kb) K_0(kr) \right) e^{ikx},$$

123 and the central equation (2.10) simplifies to its axisymmetric form

$$124 \quad \int_{-L}^L kS \left[iS_t \left(K_1(kb) I_0(kS) + I_1(kb) K_0(kS) \right) \right. \\ 125 \quad \left. + q_x \left(K_1(kb) I_1(kS) - I_1(kb) K_1(kS) \right) \right] e^{ikx} dx = 0.$$

127 Following Wilkening & Vasan [21] we may write this as

$$128 \quad \int_{-L}^L e^{ikx} S \left(K_1(kb) I_0(kS) + I_1(kb) K_0(kS) \right) \mathcal{N}(x) dx \\ 129 \quad (2.13) \quad = \int_{-L}^L i e^{ikx} S \left(K_1(kb) I_1(kS) - I_1(kb) K_1(kS) \right) \partial_x \mathcal{D}(x) dx,$$

131 where $\mathcal{D}(x) \equiv q(x)$ is the Dirichlet surface data, and $\mathcal{N}(x) \equiv S_t$ is the Neumann
132 surface data. As was pointed out by Wilkening & Vasan [21] this implicitly assumes
133 that it is possible to connect the Dirichlet and Neumann data via an infinite series
134 expansion in terms of the basis functions (2.11); for the two-dimensional case see
135 equations (2.5), (2.6) of [21].

136 Written in terms of the surface variables, the axisymmetric form of Bernoulli's
137 equation (2.2) is given by

$$138 \quad (2.14) \quad q_t + \frac{1}{2} q_x^2 - \frac{1}{2} \frac{(S_t + S_x q_x)^2}{1 + S_x^2} + \frac{\gamma \kappa}{\rho} - V = \mathcal{E}(t).$$

139 Equations (2.12) and (2.14) constitute the equations of motion for the problem ex-
140 pressed in terms of surface variables only.

141 **2.1. Travelling-wave solutions.** To compute travelling-wave solutions we in-
 142 troduce the change of variables $(x, t) \mapsto (z, t)$, where $z = x - ct$ for constant wave
 143 speed $c > 0$. In the new variables, the Bernoulli condition (2.14) becomes

$$144 \quad (2.15) \quad q_t - cq_z + \frac{1}{2}q_z^2 - \frac{1}{2} \frac{(S_t - cS_z + S_zq_z)^2}{1 + S_z^2} + \frac{\gamma\kappa}{\rho} - V = \mathcal{E}.$$

145 Henceforth we seek only fixed-form travelling wave solutions in which case $S_t = q_t = 0$.
 146 Introducing the travelling-wave change of variables into (2.12) we observe, as did De-
 147 coninck & Oliveras [8] for two-dimensional flow, that the resulting form can be sim-
 148 plified further using integration by parts. First noting the relations (e.g. Abramowitz
 149 & Stegun [2], p. 376)

$$150 \quad (2.16) \quad \frac{1}{\xi} \frac{d}{d\xi} (\xi I_1(\xi)) = I_0(\xi), \quad \frac{1}{\xi} \frac{d}{d\xi} (\xi K_1(\xi)) = -K_0(\xi),$$

151 we integrate the first integral in (2.12) by parts to obtain

$$152 \quad (2.17) \quad \int_{-L}^L kS(q_z - c) \left(K_1(kb)I_1(kS) - I_1(kb)K_1(kS) \right) e^{ikz} dz = 0.$$

154 Following Deconinck & Oliveras [8], we view the Bernoulli condition (2.15) as a
 155 quadratic equation for q_z , solve accordingly, and insert the solution into (2.17) to
 156 obtain the final travelling-wave form

$$157 \quad (2.18) \quad \int_{-L}^L kS \left[(1 + S_z^2)(c^2 - 2\mathcal{F}) \right]^{1/2} \left(K_1(kb)I_1(kS) - I_1(kb)K_1(kS) \right) e^{ikz} dz = 0,$$

159 where

$$160 \quad (2.19) \quad \mathcal{F} \equiv \frac{\gamma\kappa}{\rho} - V - \mathcal{E}, \quad \kappa = -\frac{S_{zz}}{(1 + S_z^2)^{3/2}} + \frac{1}{S(1 + S_z^2)^{1/2}}.$$

161 We recall that $k = n\pi/L$ with $n = \pm 1, \pm 2, \dots$. Note that (2.18) is trivially satisfied
 162 when $k = 0$.

163 **3. Travelling-waves on a ferrofluid column.** Having established the basic
 164 equations of motion for cylindrical geometry, we next demonstrate how the formula-
 165 tion can be applied to a particular case study. The flow domain Ω is as described in
 166 section 2, and is assumed to be filled with a ferrofluid which experiences a body force
 167 when subjected to a magnetic field (e.g. Rosensweig [16]). The region $0 \leq r \leq b$ is
 168 occupied by a metallic rod carrying an electric current I in the positive x direction.
 169 Such a configuration has been realised in experiments (e.g. Bourdin *et al.* [7]). The
 170 current generates an azimuthal magnetic field $\mathbf{H} = I\mathbf{e}_\theta/(2\pi r)$. The magnetic body
 171 force in the fluid is (e.g. Rosensweig [16])

$$172 \quad (3.1) \quad \chi\mu_0\mathbf{H} \cdot \nabla\mathbf{H} = -\frac{\mu_0\chi I^2}{4\pi^2 r^3} \mathbf{e}_r,$$

173 where χ is the magnetic susceptibility of the ferrofluid and $\mu_0 = 4\pi \times 10^{-7} \text{Hm}^{-1}$ is
 174 the magnetic permeability in a vacuum. The corresponding potential field associated
 175 with this force is

$$176 \quad (3.2) \quad V = \frac{\mu_0\chi I^2}{8\pi^2 r^2}.$$

177 The magnetic field stabilises the ferrofluid column against the well-known Rayleigh-
 178 Plateau instability (e.g. Drazin & Reid [11]) so that, in the absence of surface distur-
 179 bances, it adopts an equilibrium configuration with $S = a$, for constant a . Henceforth
 180 we nondimensionalise variables using a as the reference length scale and $(a^3\rho/\gamma)^{1/2}$ as
 181 the reference time scale. Non-dimensionalising in this way reveals the importance of
 182 two dimensionless parameters, namely the dimensionless rod radius and the magnetic
 183 Bond number,

$$184 \quad (3.3) \quad b^* = \frac{b}{a}, \quad B = \frac{\mu_0\chi I^2}{4\pi^2\gamma a}.$$

185 Henceforth we drop the asterisk on b^* for convenience.

186 In dimensionless form, the central equations (2.18), (2.19) become

$$187 \quad (3.4) \quad \int_{-L}^L kS \left[(1 + S_z^2) \left(\frac{c^2}{2} - \frac{1}{S(1 + S_z^2)^{1/2}} + \frac{S_{zz}}{(1 + S_z^2)^{3/2}} + \frac{B}{2S^2} + \mathcal{E} \right) \right]^{1/2}$$

$$188 \quad \times \left(K_1(kb)I_1(kS) - I_1(kb)K_1(kS) \right) e^{ikz} dz = 0,$$

189 where c and S are now dimensionless

190 Blyth & Părau [6] computed fully nonlinear solitary wave solutions for this fer-
 191 rofluid system. Doak & Vanden-Broeck [10] computed periodic waves and generalised
 192 solitary waves. In relating the results to be presented below with those found by
 193 Blyth & Parau (2014), we take the Bernoulli constant in (2.15) to be

$$195 \quad (3.5) \quad \mathcal{E} = 1 - \frac{B}{2}.$$

196 In making a correspondence between the present work and that of Blyth & Părau [6],
 197 it is important to note that the transformation $\phi_z \mapsto \phi_z - c$ is required to map from
 198 the velocity potential used here to that adopted by BP (this explains the absence of
 199 the term $c^2/2$ seen on the right hand side of BP's (3.5) with the choice made in (3.5)
 200 for the Bernoulli constant).

201 Linearising (2.18) it is straightforward to show that small amplitude waves with
 202 wavenumber $k_1 = \pi/L$ propagate on the surface of the ferrofluid column with speed
 203 c_0 given by (see Arkhipenko & Barkov [3]; Blyth & Părau [6])

$$204 \quad (3.6) \quad c_0^2 = \frac{1}{k_1} \left(\frac{I_1(k_1)K_1(k_1b) - I_1(k_1b)K_1(k_1)}{I_1(k_1b)K_0(k_1) + I_0(k_1)K_1(k_1b)} \right) (k_1^2 - 1 + B).$$

205 **3.1. Numerical method.** In practice we solve for free surface profiles $S(z)$ that
 206 satisfy (2.18) using a numerical method. The form (2.18) has been derived assuming
 207 periodicity with period L . Accordingly we seek periodic travelling-wave solutions as
 208 a Fourier expansion. With a view to numerical implementation we write

$$209 \quad (3.7) \quad S(z) \approx S_N = \sum_{n=-N}^N a_n e^{in\pi z/L}$$

210 for some specified level of truncation N , where the constant generally complex coeffi-
 211 cients a_n are to be found. Note that since $S(z)$ is real, we must have that $a_n = a_{-n}^*$.
 212 For a wave that is even about $z = 0$ the coefficients a_n are real and in this case we

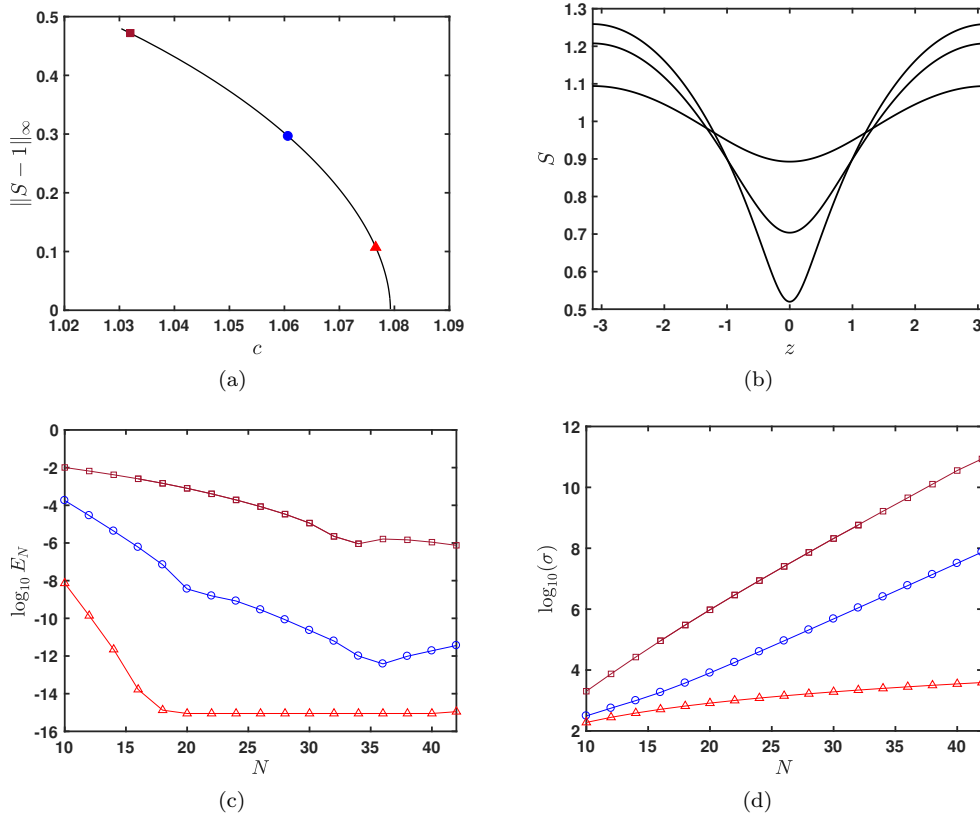


FIG. 2. A solution branch for periodic waves of period $2L = 2\pi$ when $B = 1.5$ and $b = 0.1$: (a) the infinity norm $\|S - 1\|_\infty$ against the wave speed c . The symbols correspond to $\|S - 1\|_\infty = 0.107$ ($a_2 = 0.05$) [light red \triangle], 0.296 ($a_2 = 0.12$) [blue \circ] and 0.479 ($a_2 = 0.16$) [dark red \square]; (b) the wave profiles corresponding to the symbols on the branch in (a); (c) the Cauchy error $E_N = \|S_N - S_{N-2}\|_2$ at the symbols in (a); (d) the condition number $\sigma(J)$ against N for each symbol in (a).

213 may replace $\exp(ikz)$ with $\cos kz$ to given an entirely real expression in (2.18). All of
 214 the waves to be presented below possess this symmetry.

215 Substituting (3.7) into (2.18) we approximate the resulting integral using the pe-
 216 riodic trapezium rule over a grid of equally-spaced points in the interval $[-L, L - h]$
 217 with $h = 2L/(2N + 1)$. We note that the periodic trapezium rule delivers exponen-
 218 tial accuracy as is discussed by Trefethen & Weideman [17]. Derivatives of S are
 219 computed spectrally by taking a fast Fourier transform; products of derivatives are
 220 computed in real space. We use the zero-padding technique to mitigate against alias-
 221 ing error. Setting $k = n\pi/L$ we pick n from each value in the discrete set $\{1, \dots, N/2\}$
 222 to obtain $2N$ algebraic equations for the $2N + 2$ unknowns comprising the $2N + 1$
 223 Fourier coefficients a_n and c . A further condition comes from fixing the mean radius
 224 of the ferrofluid column so that $a_0 = 1$. One more equation is needed, and in practice
 225 we enforced a non-zero value of the second Fourier coefficient a_2 to ensure a wave of
 226 non-zero amplitude. This yields a set of $2N + 2$ algebraic equations for the $2N + 2$
 227 unknowns which is solved using Newton's method for which the Jacobian J is com-
 228 puted numerically. All of the computations, including the calculation of the modified
 229 Bessel functions, were done in Matlab. [To attempt to maintain a well-scaled Jacobian](#)

230 J we divided the integrand in (2.18) by its maximum value over one period. Further
 231 discussion on this point can be found below.

232 As a test of our numerical procedure we repeated the two-dimensional calculations
 233 of Deconinck & Oliveras [8] using a modified form of our own code. Tests on the
 234 accuracy of the results in axisymmetry will be discussed in the next section. We also
 235 successfully recomputed some of the solitary wave solutions presented by Blyth &
 236 Părau [6].

237 **3.2. Results.** In keeping with our intention to demonstrate the efficacy of the
 238 AFM method for axisymmetric geometry, in the following two subsections we outline
 239 its capability for computing nonlinear periodic waves and solitary waves on a ferrofluid
 240 column. We note that nonlinear solutions for both periodic and solitary waves have
 241 been studied in detail elsewhere (see Doak & Vanden-Broeck [10] and Blyth & Părau
 242 [6]) using finite-difference methods.

243 **3.2.1. Periodic waves.** We may compute periodic waves using the numerical
 244 method described in section 3.1. In practice we latch onto a periodic solution branch
 245 by first computing a small amplitude wave using (3.6) to provide an initial guess for
 246 c (for chosen wavelength L) to be used in Newton's method.

247 Figure 2 shows a sample set of calculations for the branch of periodic waves of
 248 half-period $L = \pi$ for the case $B = 1.5$, $b = 0.1$. Panel (a) shows the solution
 249 branch characterised by the infinity norm $\|S - 1\|_\infty$ that bifurcates from the linear
 250 wave speed $c_* = 1.079$. Evidently the wave speed decreases along the branch so
 251 that $c < c_*$ for the nonlinear waves. Typical wave profiles along the branch are
 252 shown in panel (b). Numerical difficulties prevent continuation along the branch
 253 to smaller wave speeds than those shown in the figure. Ultimately we expect the
 254 waves to pinch together in the trough region to form trapped bubbles (see Doak &
 255 Vanden-Broeck [10]), similar to those seen in two-dimensional capillary and capillary-
 256 gravity waves. Since it is restricted to functions $S(z)$ which are single-valued in z it
 257 is not possible to capture such solutions with the present formulation. However as
 258 was pointed out by Wilkening & Vasan [21] for two-dimensional problems, the AFM
 259 method suffers from some ill-conditioning which appears to be the primary obstacle
 260 which frustrates continuation to larger amplitude. In particular the issue is connected
 261 with the possibility of identifying an infinite series representation for the Dirichlet and
 262 Neumann data in (2.13). In panel (c) we show the L_2 -norm $E_N = \|S_N - S_{N-2}\|_2$
 263 for increasing truncation level N . While Cauchy convergence is demonstrated for
 264 the smallest amplitude wave shown (i.e. for $a_2 = 0.05$) down to machine accuracy
 265 using double precision arithmetic, the same convergence cannot be achieved for the
 266 larger amplitude waves. The condition number $\sigma(J)$ of the Jacobian matrix J at the
 267 converged solution is plotted versus the truncation level N in panel (d) of figure 2,
 268 and it appears to be growing exponentially for the larger amplitude waves. Wilkening
 269 & Vasan [21] noted how to overcome this issue via a regularisation technique but we
 270 have not attempted to follow this here.

271 Figure 3(a) shows another example of a nonlinear periodic wave computed using
 272 the present method for the shorter domain $2L = \pi$ for $B = 30$ and $b = 0.1$. When
 273 the magnetic Bond number B exceeds a critical value $B_2(b)$ which depends on the
 274 rod radius, the dispersion curve for small amplitude periodic waves $c_0(k)$ versus k
 275 has a minimum (Blyth & Părau [6] – see their figure 1a). This raises the prospect
 276 of small amplitude periodic waves with two or more resonant wavenumbers for the
 277 same wave speed; this is the well-known phenomenon of Wilton ripples (e.g. Vanden-
 278 Broeck [18]). Solutions of this type can also be captured using the current method (we

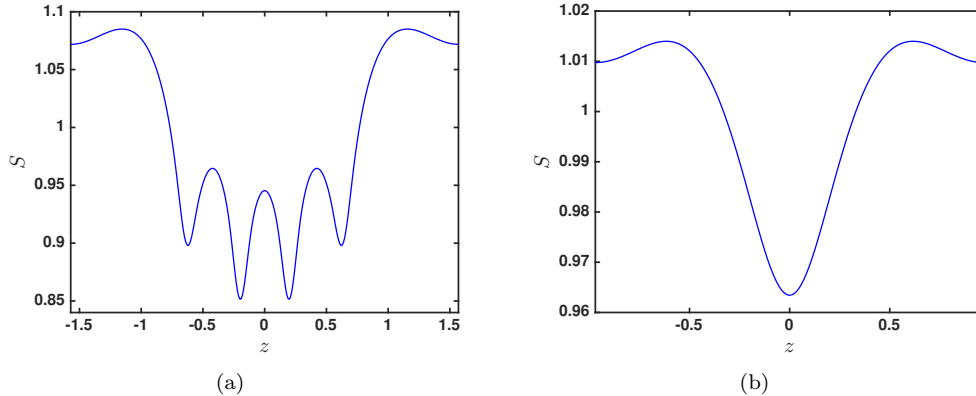


FIG. 3. (a) Periodic wave for $B = 30$ and $b = 0.1$ with $2L = \pi$ and $c = 3.301$. (b) A periodic waves with Wilton ripples for $B = 30$ and $b = 0.1$ and $c = 3.097$ with $2L = 2.061 = 2\pi/k_1$ (with $k_1 = 3.2375$).

279 note that Doak & Vanden-Broeck [10] have recently computed solutions with Wilton
 280 ripples on a ferrofluid jet using a finite difference approach). In figure 3(b) we show
 281 an example of such a solution for $b = 0.1$ and $B = 30 > B_2(0.1) \approx 9$ with a 1:2
 282 resonance meaning that linear waves with wavenumbers k_1 and $2k_1$ exist for the same
 283 wave speed c . Using the the linear theory result (3.6) we find that this occurs when
 284 $k_1 = 3.2375$ and $c = 3.173$. The solution shown in figure 3(b) lies on the solution
 285 branch which bifurcates from this point and is shown for the wave speed $c = 3.097$.

286 **3.2.2. Solitary waves.** Solitary wave solutions have previously been computed
 287 by Rannacher & Engel [15] using a weakly-nonlinear KdV model and by Blyth &
 288 Părău [6] for the fully nonlinear system. The latter authors noted that solitary waves
 289 solutions arise as bifurcations from the small amplitude periodic wave solution or
 290 as nonlinear bifurcations starting at finite amplitude. The character of the possible
 291 solitary wave solutions depends on the value of B . Indeed Blyth & Părău [6] showed
 292 that elevation solitary waves (with $S(0) > 1$) are possible in the ranges $1 < B < 2$
 293 and $B > B_2(b)$, where the threshold value $B_2(b)$ has a closed form expression and is
 294 such that $B_2 \rightarrow 9$ as $b \rightarrow 0$. Depression solitary wave solutions (with $S(0) < 1$) are
 295 found for all $B > 1$.

296 We may compute solitary waves using the AFM method as follows: first we follow
 297 the branch of periodic waves emanating from small amplitude where the wave speed
 298 c satisfies (3.6); having identified a wave of some amplitude, we extend the domain
 299 L by continuation to an appropriately large value; finally, noting that our numerical
 300 procedure fixes the mean level of $S(z)$ so that in general we have attained a solitary
 301 wave with $S(\pm\infty) \neq 1$, we elevate the far-field level by continuation until $S(\pm\infty) = 1$.
 302 Figure 4(a) shows an elevation solitary wave computed in this way for $B = 1.25$ and
 303 $b = 0.1$. An example of a depression solitary wave is shown in figure 4(b). Also shown
 304 on the same graph, and barely distinguishable from the present solution, is the same
 305 wave computed using the finite difference approach of Blyth & Părău [6] (see their
 306 figure 5a).

307 As was noted in section 3.2.1 when $B > B_2(b)$ the linear dispersion curve has
 308 a minimum. As demonstrated by Groves & Nilsson [12] the nonlinear Schrödinger
 309 equation is a good approximation in the vicinity of this minimum and this equation

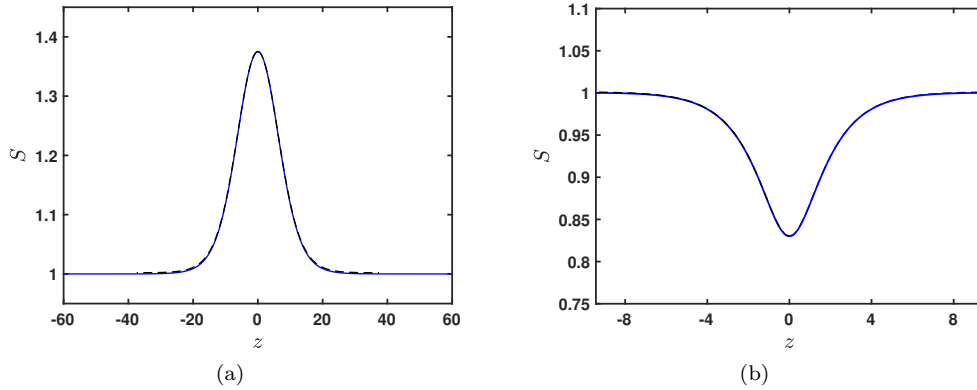


FIG. 4. (a) Elevation solitary wave solution for $B = 1.25$ and $b = 0.1$, and (b) Depression solitary wave for $B = 4$ and $b = 0.1$. In both panels the solid line is the result computed using the present method, and the broken line is the solution of Blyth & Părău [6] shown in their figure 5a (for panel a) and their figure 6 (for panel b).

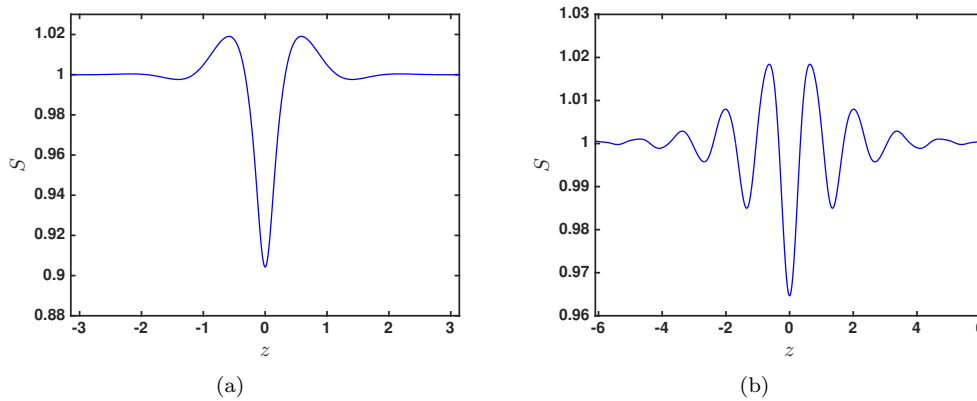


FIG. 5. Depression solitary waves (with $S(0) < 1$) on a branch bifurcation from the minimum of the linear dispersion curve for $B = 30$ and $b = 0.1$. (a) $c = 2.918$ and (b) $c = 3.085$.

310 has both elevation and depression solitary waves. Fully nonlinear solutions of both
 311 of these types were computed by Blyth & Părău [6]. Examples of depression waves
 312 of this type computed using the present AFM method are shown in figure 5. In
 313 particular the wave in panel (a) is a reproduction using the current method of that
 314 shown in figure 9(a) of Blyth & Părău [6].

315 **4. Summary.** We have developed an AFM (Ablowitz-Fokas-Musslimani) water-
 316 wave method for cylindrical geometry, and have demonstrated the use of the method
 317 for computing fully nonlinear travelling-waves on a ferrofluid column which has been
 318 stabilised by an azimuthal magnetic field. Previous studies have used finite-difference
 319 methods based on a hodograph-type approach which simplifies the domain geometry
 320 but which requires the solution of a nonlinear equation for the velocity potential.
 321 A significant drawback of such methods is that they require the discretisation of
 322 the entire fluid domain. In contrast the AFM method is formulated with reference
 323 to variables evaluated at the free surface only. [While the finite-difference approach](#)

324 produces a discretisation error which depends algebraically on the mesh size of the
 325 computational grid, the AFM method is much simpler to implement and can achieve
 326 exponential convergence. However, as was noted above, and discussed in depth for
 327 the two-dimensional case by Wilkening and Vasan [21], the method can suffer from
 328 ill-conditioning and regularisation techniques may be needed for very high precision
 329 calculations. Nonetheless, as we have demonstrated, even for relatively large ampli-
 330 tude waves, a good degree of accuracy can be achieved. Moreover, the method can be
 331 readily adapted for investigating the stability of travelling-wave solutions, as was done
 332 in two-dimensions by Deconinck & Oliveras [8]. For the axisymmetric computations
 333 performed here this is left as a topic for future work.

334

REFERENCES

- 335 [1] M. J. ABLOWITZ, A. S. FOKAS, AND Z. H. MUSSLIMANI, *On a new non-local formulation of*
 336 *water waves*, J. Fluid Mech., 562 (2006), pp. 313–343.
- 337 [2] M. ABRAMOWITZ AND I. A. STEGUN, *Handbook of mathematical functions: with formulas,*
 338 *graphs, and mathematical tables*, vol. 55, Dover publications New York, 1972.
- 339 [3] V. I. ARKHIPENKO AND Y. D. BARKOV, *Experimental study of the breakdown of the cylindrical*
 340 *layer of a magnetizable fluid under the action of magnetic forces*, J. Appl. Mech. Tech.
 341 Phys, 21 (1980), pp. 98–105.
- 342 [4] A. C. L. ASHTON AND A. S. FOKAS, *A non-local formulation of rotational water waves*, J.
 343 Fluid Mech., 689 (2011), pp. 129–148.
- 344 [5] V. BASHTOVOL, A. REX, AND R. FOIGUEL, *Some non-linear wave processes in magnetic fluid*,
 345 Journal of Magnetism and Magnetic Materials, 39 (1983), pp. 115–118.
- 346 [6] M. G. BLYTH AND E. I. PĂRĂU, *Solitary waves on a ferrofluid jet*, J. Fluid Mech., 750 (2014),
 347 pp. 401–420.
- 348 [7] E. BOURDIN, J.-C. BACRI, AND E. FALCON, *Observation of axisymmetric solitary waves on the*
 349 *surface of a ferrofluid*, Phys. Rev. Lett., 104 (2010), p. 094502.
- 350 [8] B. DECONINCK AND K. OLIVERAS, *The instability of periodic surface gravity waves*, J. Fluid
 351 Mech., 675 (2011), pp. 141–167.
- 352 [9] B. DECONINCK AND O. TRICHTCHENKO, *Stability of periodic gravity waves in the presence of*
 353 *surface tension*, Eur. J. Mech. B/Fluids, 46 (2014), pp. 97–108.
- 354 [10] A. DOAK AND J.-M. VANDEN-BROECK, *Travelling wave solutions on an axisymmetric ferrofluid*
 355 *jet*, Submitted.
- 356 [11] P. G. DRAZIN AND W. H. REID, *Hydrodynamic stability*, Cambridge university press, 2004.
- 357 [12] M. GROVES AND D. NILSSON, *Spatial dynamics methods for solitary waves on a ferrofluid jet*,
 358 J. Math. Fluid Mech., (2018), pp. 1–32.
- 359 [13] T. S. HAUT AND M. J. ABLOWITZ, *A reformulation and applications of interfacial fluids with*
 360 *a free surface*, J. Fluid Mech., 631 (2009), pp. 375–396.
- 361 [14] D. LANNES, *The water waves problem: mathematical analysis and asymptotics*, vol. 188, Amer-
 362 ican Mathematical Soc., 2013.
- 363 [15] D. RANNACHER AND A. ENGEL, *Cylindrical korteweg–de vries solitons on a ferrofluid surface*,
 364 New J. Phys., 8 (2006), p. 108.
- 365 [16] R. E. ROSENSWEIG, *Ferrohydrodynamics*, Courier Corporation, 2013.
- 366 [17] L. N. TREFETHEN AND J. A. C. WEIDEMAN, *The exponentially convergent trapezoidal rule*,
 367 SIAM Review, 56 (2014), pp. 385–458.
- 368 [18] J.-M. VANDEN-BROECK, *Gravity-capillary free-surface flows*, Cambridge University Press, 2010.
- 369 [19] J.-M. VANDEN-BROECK, T. MILOH, AND B. SPIVACK, *Axisymmetric capillary waves*, Wave
 370 motion, 27 (1998), pp. 245–256.
- 371 [20] V. VASAN AND B. DECONINCK, *The inverse water wave problem of bathymetry detection*, J.
 372 Fluid Mech., 714 (2013), pp. 562–590.
- 373 [21] J. WILKENING AND V. VASAN, *Comparison of five methods of computing the dirichlet-neumann*
 374 *operator for the water wave problem*, Contemp. Math, 635 (2015), pp. 175–210.